AFOSR 66-0500 Contract AF 49(638)-1391

895

HYPERSONIC FLOW ALONG TWO INTERSECTING PLANES

by

Robert J. Cresci

March 1966

POLYTECHNIC INSTITUTE OF BROOKLYN

DEPARTMENT
of
AEROSPACE ENGINEERING
and
APPLIED MECHANICS

PIBAL REPORT NO. 895

AFOSR 66-0500

HYPERSONIC FLOW ALONG TWO INTERSECTING PLANES

by

Robert J. Cresci

This study was supported by the

Air Force Office of Scientific Research

Contract AF 49(638)-1391

Polytechnic Institute of Brooklyn

Department

of

Aerospace Engineering and Applied Mechanics

March 1966

HYPERSONIC FLOW ALONG TWO INTERSECTING PLANES†

Robert J. Cresci*

Polytechnic Institute of Brooklyn, Farmingdale, New York

SUMMARY

The present paper deals with an experimental study of the viscous-inviscid interaction occuring in a corner region under hypersonic, low density, free stream conditions. The tests were conducted in the Mach 11.8 hypersonic tunnel at PIBAL over a range of free stream Reynolds numbers between 0.15×10^6 and 0.50×10^6/ft. The model consists of two sharp edged plates mounted at an angle of 90° with respect to each other and with normal leading edges. Data obtained include surface measurements of pressure and heat transfer for values of the interaction parameter ($\bar{\chi}$) between 1.0 and 20. The entire corner region is surveyed at a value of $\bar{\chi} = 2.5$ and measurements of total temperature, pitot, and static pressure are obtained.

The results indicate that the static pressure in the region of intersection of the shock layers is as much as twice that of the local two dimensional value. The local heat rates in this region are also considerably larger than their two dimensional counterparts.

---

† This research was supported by the United States Air Force through the Air Force Office of Scientific Research, under Contract No. AF 49 (638)-1391. This paper will be presented at the 1966 Heat Transfer and Fluid Mechanics Institute, University of Santa Clara, California, June 22-24, 1966.

The author is pleased to acknowledge the staff of the hypersonic facility and, in particular, Mr. C. Nardo for running the tests and analyzing the data, and Prof. M. H. Bloom for his many discussions and suggestions throughout the research program.

*Associate Professor Aerospace Engineering

BLANK PAGE

TABLE OF CONTENTS

Section		Page
I	Introduction.	1
II	Model Design and Test Procedure.	3
III	Presentation and Discussion of Data.	6
IV	Concluding Remarks.	11
V	References.	12

LIST OF ILLUSTRATIONS

Figure		Page
1	(a) Schematic Representation of Flow System.	15
	(b) Model Design and Instrumentation Details.	16
2	Photographs of Model and Survey Probes.	17
3	Flat Plate Pressure Distribution ($z \rightarrow \infty$).	18
4	Flat Plate Heat Transfer ($z \rightarrow \infty$).	19
5	Static Pressure Profile on Flat Plate, $\bar{X} = 2.5$ ($z \rightarrow \infty$). . .	20
6	Surface Pressure in Corner Region (a) $z = 0.125$ in.	21
	(b) $z = 0.250$ in.	22
	(c) $z = 0.375$ in.	23
	(d) $z = 0.500$ in.	24
	(e) $z = 1.0$ in.	25
	(f) $z = 1.5$ in.	26
7	Local Heat Transfer in Corner Region (a) $\bar{X} = 7.0$.	27
	(b) $\bar{X} = 5.7$	
	(c) $\bar{X} = 4.6$.	28
	(d) $\bar{X} = 3.6$	
	(e) $\bar{X} = 2.2$.	29
	(f) $\bar{X} = 1.9$	
8	Total Temperature Profiles in Corner Region, $\bar{X} = 2.5$. . .	30
9	Pitot Pressure Profiles in Corner Region, $\bar{X} = 2.5$.	31
10	Mach Number Distribution in Corner Region, $\bar{X} = 2.5$. . . .	32
11	Mach Number Contours in Corner Region, $\bar{X} = 2.5$.	33
12	Skin Friction Variation in Corner Region, $\bar{X} = 2.5$.	34

LIST OF SYMBOLS

C = $T_\infty \mu / T \mu_\infty$ - Chapman - Rubesin Constant

C_f = $2\tau w / \rho_\infty u_\infty^2$ - skin friction coefficient

H stagnation enthalpy

k coefficient of thermal conductivity

M Mach number

p pressure

q = $(k \partial T / \partial y)_w$ - heat transfer rate

Re_x = $\rho u x / \mu$ - Reynolds number

St = $q_w / \rho_\infty u_\infty (H_\infty - H_w)$ - Stanton number

T temperature

u velocity in the streamwise direction

x coordinate in the streamwise direction

z coordinate along horizontal surface normal to x axis

y coordinate along vertical surface normal to x axis

δ boundary layer thickness

ρ mass density

τ $(\mu \partial u / \partial y)_w$ - shear stress

μ coefficient of viscosity

$\bar{\chi}$ = $M_\infty^3 \sqrt{C / Re_{x_\infty}}$ - Viscous - inviscid interaction parameter

Subscripts

e conditions external to the boundary layer

s stagnation conditions

w conditions evaluated at the surface

$z \rightarrow \infty$, 2D } flat plate conditions (no corner)

∞ free stream conditions

I. INTRODUCTION

The flow along two intersecting planes, which form an interior corner aligned with respect to the free stream direction, represents a basic flow configuration of interest both to the applied and the theoretical fluid dynamicist. This problem has applications with respect to the intersection of typical fuselages and lifting or control surfaces of high speed flight vehicles. As a result, there has been a reasonable amount of literature generated with respect to various aspects of this flow system.

The inviscid flow field generated by such geometries has been studied quite extensively in the supersonic flow regime, cf. references (1) through (4), for planar surfaces intersecting at right angles with each other. The associated viscous flow problem of a three dimensional boundary layer in a corner has also been investigated in some detail in references (5) through (8), for example. In the majority of these studies, the interactions in the flow and the resulting interference effects are either of a purely inviscid type or are due to the viscous interactions produced by the three dimensionality of the corner boundary layer. Reference (9) presents a preliminary comprehensive study of a combined viscous-inviscid flow interaction in a corner. The primary interest therein is directed toward the hypersonic, low density flow regime wherein the inviscid shock layer and the viscous boundary layer thickness produced under these conditions are of the same order of magnitude. In this case, the viscous and inviscid effects are interrelated and cannot be treated independently. It is evident that for these conditions, the corner flow is represented by a complex interaction between the induced inviscid field, including intersections of cylindrical shock surfaces, and the three dimensional, compressible boundary layer generated in the corner. Reference (10) presents some preliminary experimental surface pressure

data obtained in helium under hypersonic conditions and reference (4) presents some heat transfer data obtained at a Mach number of 8.0. The latter yields data in the weak interaction regime ($\bar{\chi} \sim 1.0$) on a sharp flat plate, and thus provides some basic information on the combined viscous-inviscid interaction problem.

The present study represents an experimental investigation of the hypersonic, low density flow in a corner, at a free stream Mach number of 11.8 and somewhat lower Reynolds numbers than those achieved in previous tests; figure 1(a) presents a schematic diagram of the flow system. Although a theoretical treatment of this problem is as yet unavailable, (indeed, even the more simple uncoupled viscous or inviscid problems have not yet been solved in general form) the present investigation yields some interesting details about the overall behavior that can be useful in determining a theoretical model of the flow pattern in this region. Surface measurements of pressure and heat transfer are obtained for various distances from both the leading edge and the corner intersection. The value of the hypersonic interaction parameter ($\bar{\chi} = M_\infty^3 \sqrt{C/Re_{x_\infty}}$) achieved in these tests varies between approximately one and twenty. At large lateral distances from the corner, the results compare favorably to the usual two dimensional analyses corresponding to the strong and weak interaction regimes. In addition to these measurements, the corner region is surveyed in a plane parallel to the leading edges at a value of $\bar{\chi} = 2.5$. Total temperature, and pitot probes are utilized in this survey and resulting plots of Mach number, velocity, and temperature are obtained.

The following sections describe the model design, test apparatus and procedure, a detailed exposition of the results, and finally the major conclusions derived from this study.

II. MODEL DESIGN AND TEST PROCEDURE

The test model consists of two sharp flat plates mounted normal to each other with the line of intersection aligned with respect to the free stream. A schematic of the model showing instrumentation details and locations is shown in figure (1) and photographs of the model as installed in the tunnel are presented in figure (2). As seen in the photographs, the model is sting mounted in the Mach 11.8 blowdown tunnel of the Polytechnic Institute of Brooklyn, Aerospace Laboratory. The tests were conducted over a range of free stream Reynolds numbers varying between 0.15×10^6/ft. and 0.5×10^6/ft. The tunnel stagnation temperature varied between 1700°R and 1900°R which produced a variation in the ratio of wall to stagnation temperature (Tw/Ts_∞) between 0.29 and 0.32.

The pressure instrumentation consists of flush taps with the transducers mounted directly on the inside of the plate. This is done to minimize the transducer response time since the total test time of the hypersonic tunnel is on the order of two to four seconds. With this system, the gauges respond in a fraction of a second to their steady state values. Pitot pressures are measured by means of variable reluctance type transducers mounted on a rake as shown in figure (2). These transducers are accurate in a range between 2 and 30 millimeters of mercury; the static pressures are on the order of a few hundred microns and thus require the thermocouple type (Hastings) gauge for accurate measurements. The heat gauges consist of thin stainless steel plates inserted flush with the model surface. Fine thermocouple wire is spot welded to the inner surface and the rate of temperature change is thus directly related to the local heat transfer. Due to the relatively short test time,

the heat transfer meters did not reach a high temperature and the entire model surface can be considered essentially isothermal. Both the pressure taps and the heat transfer gauges were installed in two rows parallel to the line of intersection of the model. The moveable vertical fin is then adjusted so that the local pressure and heat transfer is obtained at different distances from the corner region by utilizing the same instrumentation; this increasesthe measurement accuracy since any error in calibration or gauge behavior is consistent for all locations of the gauge from the corner.

In order to obtain the viscous-interaction effect on a purely two dimensional surface, the model was first tested with the fin removed. Since both rows of pressure taps as well as heat transfer gauges are asymmetrically located on the plate surface, this test also establishes that there are no edge effects in the region in which the measurements are taken. A row of heat gauges is also located on the fin to verify the symmetry of the corner flow about the intersection line. Since these gauges are a fixed distance from the corner, they are also indicative of the flow uniformity as the fin is moved across the plate surface.

In addition to the surface measurements, a survey of the entire corner region was taken which includes the boundary layer as well as the shock layer. Pitot pressure, static pressure, and total temperature rakes are used in this survey. The total temperatures are measured by open tip probes utilizing thermocouple wires 0.001 inches in diameter, and with an unsupported length of 0.30 inches. This was found to be sufficient to eliminate all conduction effects at the supports. These probes also provide a sufficiently rapid response time to obtain steady temperature measurements. An attempt was made to determine the

local static pressure in the corner region by using static probes; this data was found to be inconclusive due partially to the low pressures (and correspondingly long response time) and mainly to the high sensitivity of the probes to the flow alignment. All data was recorded on recording potentiometers throughout the duration of the test.

III. PRESENTATION AND DISCUSSION OF DATA

The flat plate without the fin was tested initially to determine the experimental surface pressure and heat transfer rates at various free stream Reynolds numbers and distances from the leading edge. Data from both rows of pressure taps and heat gauges are compared and found to be consistent within experimental accuracy. This indicates that both of the rows are sufficiently far from the edges of the plate to eliminate all of the end effects. Tests were run at three different (nominal) free stream Reynolds numbers; these range between 0.15×10^6 and 0.50×10^6/ft. The data are presented in terms of the viscous-inviscid interaction parameter, $\bar{\chi}$, so that there is an overlapping of data obtained from various surface tap locations for different Reynolds number tests.

The local surface pressure, normalized with respect to the free stream static pressure, is shown in figure (3) as a function of $\bar{\chi}$. Also included in this plot is the weak interaction theory of reference (11), and the strong interaction analyses of references (12) and (13). The data are seen to agree reasonably well with the predictions. The local Stanton number is shown in figure (4) as a function of $\bar{\chi}$ with the boundary layer predictions of reference (14) and the strong interaction analyses of references (13) and (15) included for comparison. The data is seen to be somewhat higher than the analyses predict particularly for larger values of $\bar{\chi}$. This is similar to the data trend observed in reference (16) which was obtained in a shock tunnel under cold wall conditions; the data of reference (16) is also included in this figure. Profiles of static and pitot pressure, and total temperature, were obtained by the probes described in the previous section. These are presented in figures (5), (8) and (9) for the probe located at a distance from the leading edge corresponding to a value of $\bar{\chi} = 2.5$. The static pressure

profile shown in figure (5) gives an indication of the shock location but does not accurately depict the actual static pressure variation for distances larger than roughly 3.5 inches from the surface. This is due to the shock, which is at a shallow angle, intersecting the probe at various locations along its length as the probe is moved vertically in this region. Examination of the static and pitot profiles indicates that the shock displacement occurs in the vicinity of 3.7 inches from the plate surface. In order to obtain a theoretical estimate of the shock location, the boundary layer thickness was first calculated by the method described in reference (17). At a value of $\bar{\chi} = 2.5$, this yields a thickness of 1.56 inches which is consistent with the two dimensional temperature profile of figure (8) and the pitot profile presented in figure (9). Using this displacement thickness for the effective body shape, the shock shape is determined by applying the analysis of Friedrichs, cf. reference (18), which yields a shock displacement of 3.70 inches at $\bar{\chi} = 2.5$. The agreement with the experimental location is seen to be reasonably accurate. Various blast wave analyses were applied, however, as also observed in reference (19), for example, they underestimate the shock layer thickness for plates with sharp leading edges.

The surface data obtained with the fin in position is shown in figures (6) and (7) while the boundary layer and shock profile are presented in figures (8) through (10). The surface static pressures, shown in figure (6), are normalized with respect to the free stream static as before and are plotted as function of $\bar{\chi}$ for various values of the lateral distance from the corner intersection.

The two dimensional pressure data of figure (3) are also included in figure (6) with the experimental scatter indicated by the cross hatched area. Along a line parallel to the corner intersection, and at a distance $z = 0.125''$ [figure (6a)] from the corner, the pressure is seen to be as high as twice the local two dimensional value. This ratio decreases as

$\bar{\chi}$ increases and as the distance from the corner increases, as is evident from figures (6b) through (6f). For a lateral distance approximately equal to the local two dimensional boundary layer thickness, $z \simeq 1.5''$, it is seen that for large values of $\bar{\chi}$ the pressure is essentially the two dimensional value while at lower $\bar{\chi}$, there is still a significant increase in pressure in this region. This is in contrast to the data of reference (3) wherein it was found that in a region close to the corner, the maximum pressure rise over the two dimensional value occurred at high values of $\bar{\chi}$ while at some distance from the corner, the maximum pressure increase occurred at lower $\bar{\chi}$.

In the present investigation, the maximum pressure ratio obtained is roughly two; this can be tentatively explained if one considers a particular shock configuration in the corner region. In essence, the two intersecting shocks are assumed to produce a fillet shaped shock in the vicinity of their intersection. Utilizing Newtonian theory, and applying this to the local inclination of the shock fillet with respect to the free stream, it is found that a pressure ratio of two is predicted in the corner shock layer. The lateral region over which this higher pressure will extend depends on the size of the fillet, which will increase with x if the flow in the corner region is conical as suggested in references (1) and (2). It should be noted, however, that the shock configuration assumed here is quite different from that obtained in these two references. As the distance from the leading edge, x, increases, the value of $\bar{\chi}$ decreases which is consistent with the observed data trend indicating that the higher pressure in the corner approaches the two dimensional value more rapidly with distance from the corner at higher values of $\bar{\chi}$.

Figure (7) shows the corresponding surface heat rates obtained in the corner region at various values of $\bar{\chi}$. Plots of Stanton number

vs. distance from the corner are presented and it is again evident that a large increase results in the corner region. In this case, however, the heat rate reaches a peak within the boundary layer intersection region and then decreases, approaching zero at the corner. This latter effect is consistent with the theoretical results of reference (7), for example. Increases over the local two dimensional heat transfer rates of more than 300% are observed and these also appear to be larger at the lower values of $\overline{\chi}$.

The total temperature profiles obtained in the corner region are presented in figure (8) for various distances from the plate intersection. Whereas the two dimensional profile is a monotonically increasing function, the profiles in the corner are seen to reach a peak in the vicinity of the two dimensional boundary layer edge and then decrease as the distance from the surface is further increased. Close to the corner, the profiles reach the free stream stagnation temperature more rapidly than in the two dimensional profile indicating the existence of a hot core of gas within the boundary layer interference region. Pitot pressures in the corner region are similarly presented in figure (9) for various distances from the corner. There is also seen to be a large overshoot in these profiles within the boundary layer intersection region. Using the profiles and determining a static pressure field (this was not measured in the corner region) by extrapolating the surface pressure data assuming a conical flow region, the Mach number distribution throughout the corner region is computed. These profiles are shown in figure (10). Again it is evident that there is a large velocity overshoot in the corner. The incompressible, flat plate, boundary layer analysis in a corner, cf. reference (5), predicts a velocity ratio (u/u_e) in the corner equal to the product of the two two-dimensional velocity ratios at the corres-

ponding distances in the boundary layer from each wall; this yields a monotonically increasing velocity ratio throughout the corner region. For the present test conditions, wherein the inviscid flow field is more complicated due to the shock pattern and resulting non-uniform flow, it is evident that a simplified boundary layer analysis of this type cannot predict, even qualitatively, the viscous effects in the corner region. This is readily observed in figure (11) wherein the data of figure (10) are cross plotted to give constant Mach number contours in the corner region. A large distortion of the boundary layer is seen to occur in a region on the order of the two dimensional boundary layer thickness from the corner. The contours in this area become more closely spaced, thus indicating an increase in the local shear stress. From the total temperature and Mach number distributions in the corner, the velocity distributions are computed and the surface shear stresses estimated. The accuracy of the skin friction coefficient obtained by this method is not too high but one can get a comparison between the two dimensional value and the values in the corner region. If the local skin friction is normalized with respect to the two dimensional value, the data shown in figure (12) result. It is seen that although there is a decrease in skin friction close to the corner intersection, an increase results at a distance from the corner. The effect on the overall skin friction coefficient for the entire corner configuration is not clear since the integrated effect is undetermined; it appears however that a slight increase in the total skin friction coefficient may result.

IV. CONCLUDING REMARKS

Several major conclusions may be drawn from the experimental investigation of the corner carried out under hypersonic free stream conditions. The surface data indicate that high pressure and high heat transfer rates are generated in the corner region. The heat transfer, in particular, may be a problem in any configuration design in which such a corner is utilized since increases over the two dimensional value thereof by a factor of three or four have been obtained.

The surveys of the flow field at a value of $\bar{\chi} = 2.5$ have also produced some interesting results. In particular, a localized region of high temperature, high velocity, air is found to exist in the vicinity of the intersection of the two dimensional boundary layers on the flat surfaces. These may be related to the existence of streamwise vortices that have been obtained in theoretical analyses of the boundary layer growth in a corner, e.g., reference (8). In any case, this core of high energy air tends to increase the local skin friction on the surfaces of the flat plates in this region. Although the skin friction coefficient decreases as the corner is approached, this increase farther away from the corner may be more significant, thereby resulting in an overall increase in the total skin friction coefficient of the corner configuration.

V. REFERENCES

1. Wallace, J. and Clark, J. H.: "Uniformly Valid Second-Order Solution for Supersonic Flow Over Cruciform Surfaces," Brown University, CM-1019, June 1962.
2. Hains, F.D.: "Supersonic Flow Near the Junction of Two Wedges" Jour. Aerospace Sci., Vol. 25, No. 8, pp. 530-531, August 1958.
3. Stainback, P. Calvin: "An Experimental Investigation at a Mach Number of 2.95 of Flow in the Vicinity of a 90° Interior Corner Aligned With the Free-Stream Velocity." NASA TN D-184, February 1960.
4. Stainback, P. Calvin: "Heat-Transfer Measurements at a Mach Number of 8 in the Vicinity of a 90° Interior Corner Aligned with the Free-Stream Velocity." NASA TN D-2417, August 1964.
5. Carrier, G. F.: "The Boundary Layer in a Corner." Quarterly Appl. Math., Vol. IV, No. 4, pp. 367-370, January 1947.
6. Oman, Richard, A.: "The Three-Dimensional Laminar Boundary Layer Along a Corner." Tech. Rep. No. 1 (Contract No. DA-19-020-ORD-4538), M.I.T., January 1959.
7. Bloom, M. H., Rubin, S.: "High-Speed Viscous Corner Flow." Jour. Aerospace Sci., Vol. 28, No. 2, pp. 145-157, February 1961.
8. Rubin, S.G.: "Incompressible Flow Along a Corner. Part I - Boundary Layer Solutions and Formulation of Corner Layer Problem." Polytechnic Institute of Brooklyn, PIBAL Report No. 867, AFOSR 65-1420, AD 621987, May 1965.
9. Bloom, M. H., Cresci, R. J., and Rubin, S. G.: "Viscous-Inviscid Interactions Along a Corner." AGARDograph 97, Part 2, May 1965.

10. Bogdonoff, S. M. and Vas, I. E.: "A Preliminary Investigation of the Flow in a 90° Corner at Hypersonic Speeds. Part 1 - Flat Plates with Thin Leading Edges at Zero Angle of Attack," Bell Aircraft Corporation, Purchase Order Number CRE 213078-1, December 20, 1957.

11. Lees, L. and Probstein, R. F.: "Hypersonic Viscous Flow over a Flat Plate". Report No. 195 (Contract AF 33(038)-250) Aero. Eng. Lab., Princeton University, April 1952.

12. Bertram, M. H. and Blackstock, T. A.: "Some Simple Solutions the Problem of Predicting Boundary-Layer Self-Induced Pressures." NASA TN D-798, April 1961.

13. Chan, Yat-Yung,: "Integral Methods in Compressible Laminar Boundary Layers and their Application to Hypersonic Pressure Interactions." NASA CR-284, September 1965.

14. Eckert, E. R. G.: "Survey on Heat Transfer at High Speeds," Wright Air Development Center, TR 54-70, 1954.

15. Lees, L.: "On the Boundary-Layer Equations in Hypersonic Flow and Their Approximate Solutions," Jour. Aero Sciences, Vol. 20, No. 2, pg. 143, 1953.

16. Hall, J. G. and Golian, T. C.: "Shock Tunnel Studies of Hypersonic Flat-Plate Air Flows." Cornell Aero. Lab. Report No. AD-1052-A-10, December 1960.

17. Bertram, M. W. and Feller, W. V.: "A Simple Method for Determining Heat Transfer, Skin Friction, and Boundary-Layer Thickness For Hypersonic Laminar Boundary-Layer Flows in a Pressure Gradient." NASA MEMO 5-24-59L, June 1959.

18. Sears, W.R. (Ed.): High Speed Aerodynamics and Jet Propulsion, Vol. VI, pp. 396-402, Princeton University Press, Princeton, New Jersey, 1954.

19. Harvey, W.D.: "Effects of Leading-Edge Bluntness on Pressure and Heat-Transfer Measurements over a Flat Plate." NASA TN D-2846, October 1965.

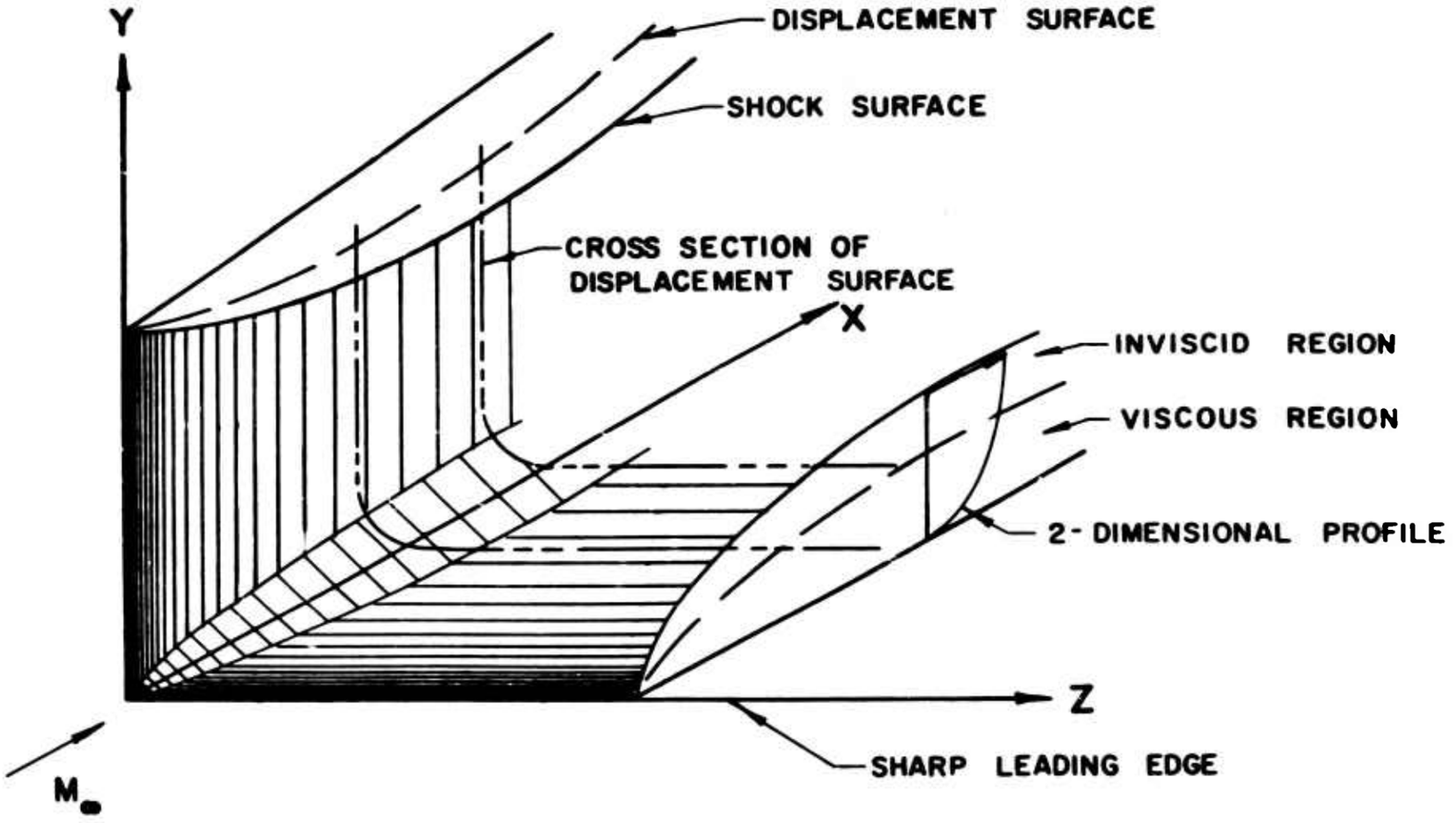

FIG. (1a) SCHEMATIC REPRESENTATION OF FLOW SYSTEM

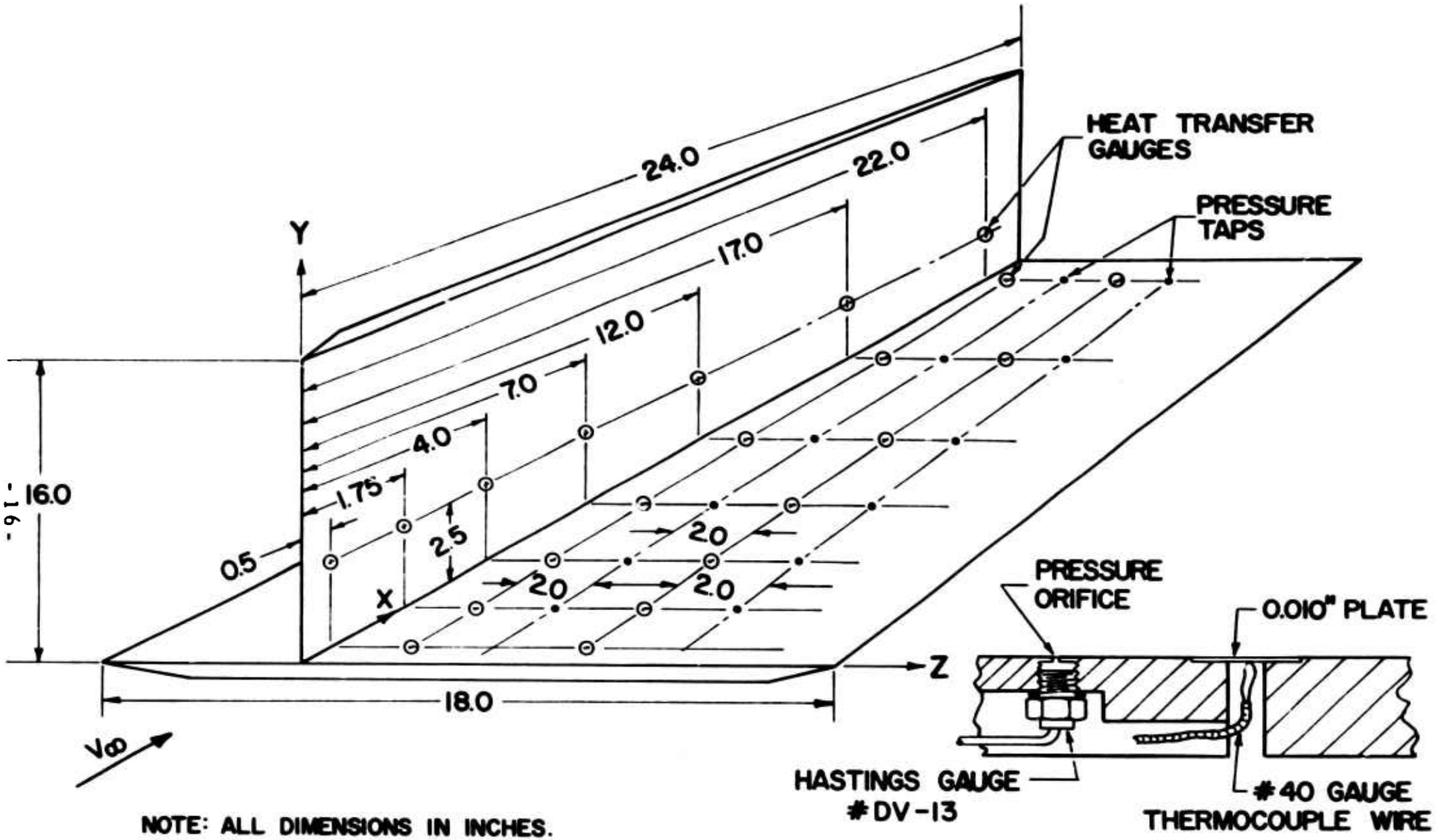

FIG. (1b) MODEL DESIGN AND INSTRUMENTATION DETAILS.

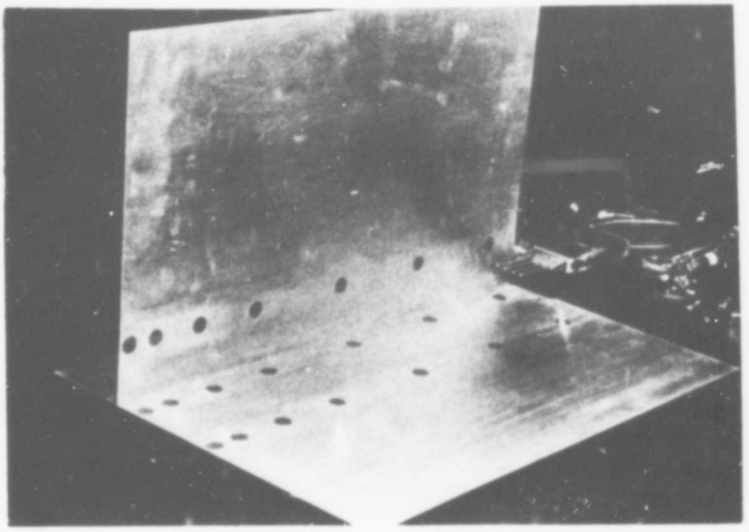

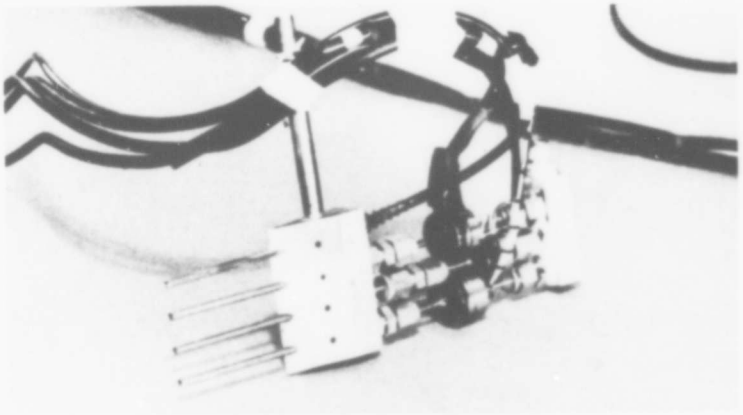

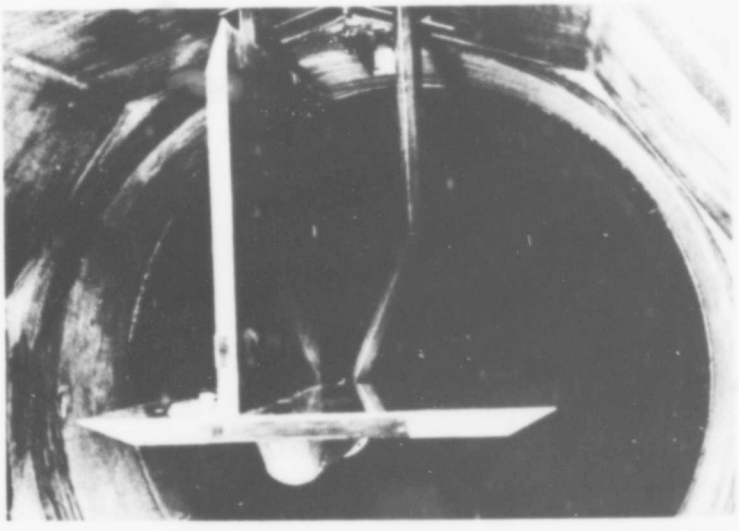

FIG. 2 PHOTOGRAPHS OF MODEL AND SURVEY PROBES.

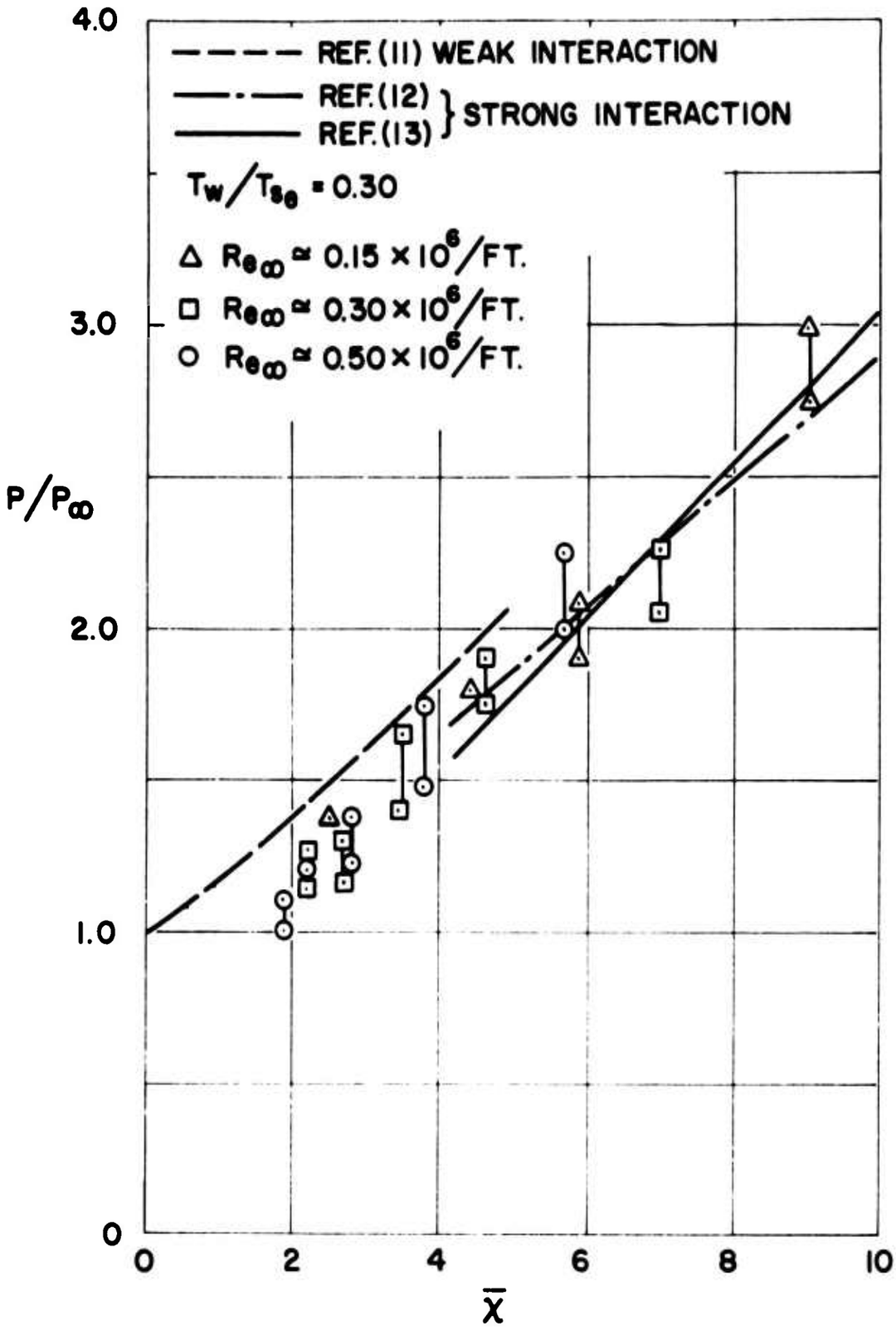

FIG. 3 FLAT PLATE PRESSURE DISTRIBUTION
$(z \rightarrow \infty)$

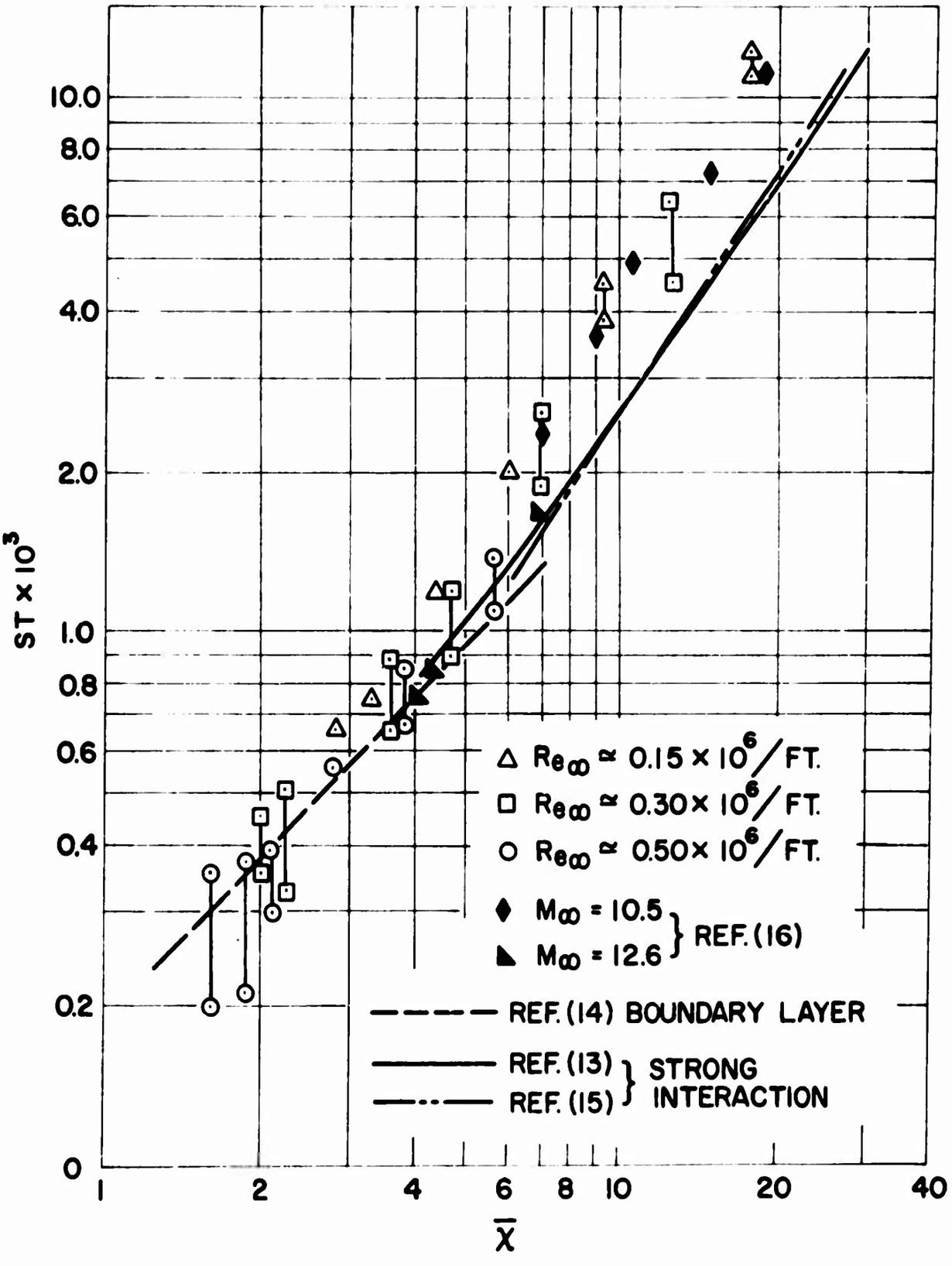

FIG. 4 FLAT PLATE HEAT TRANSFER ($z \rightarrow \infty$)

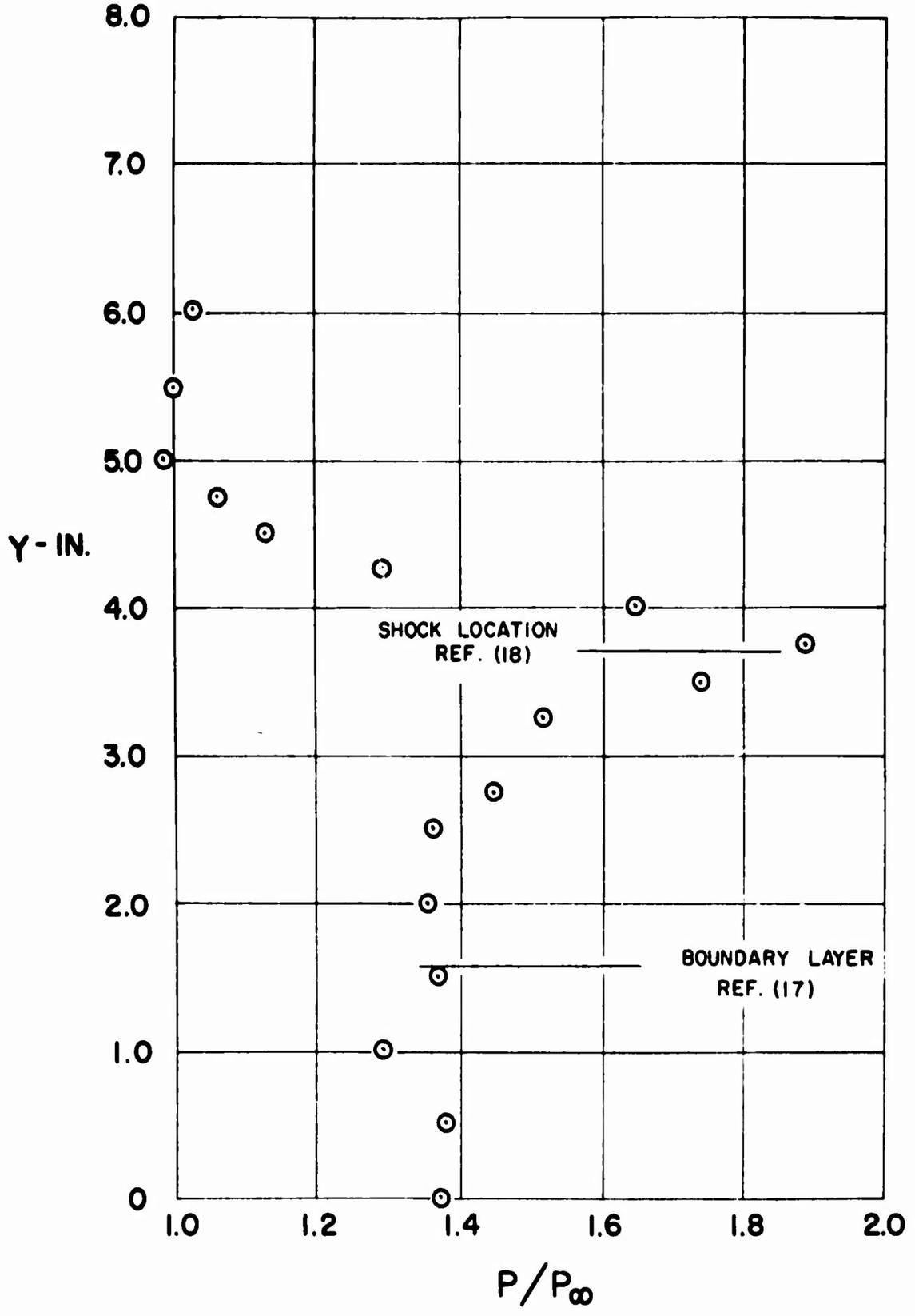

FIG. 5 STATIC PRESSURE PROFILE ON FLAT PLATE, $\bar{X} = 2.5$ $(z \to \infty)$

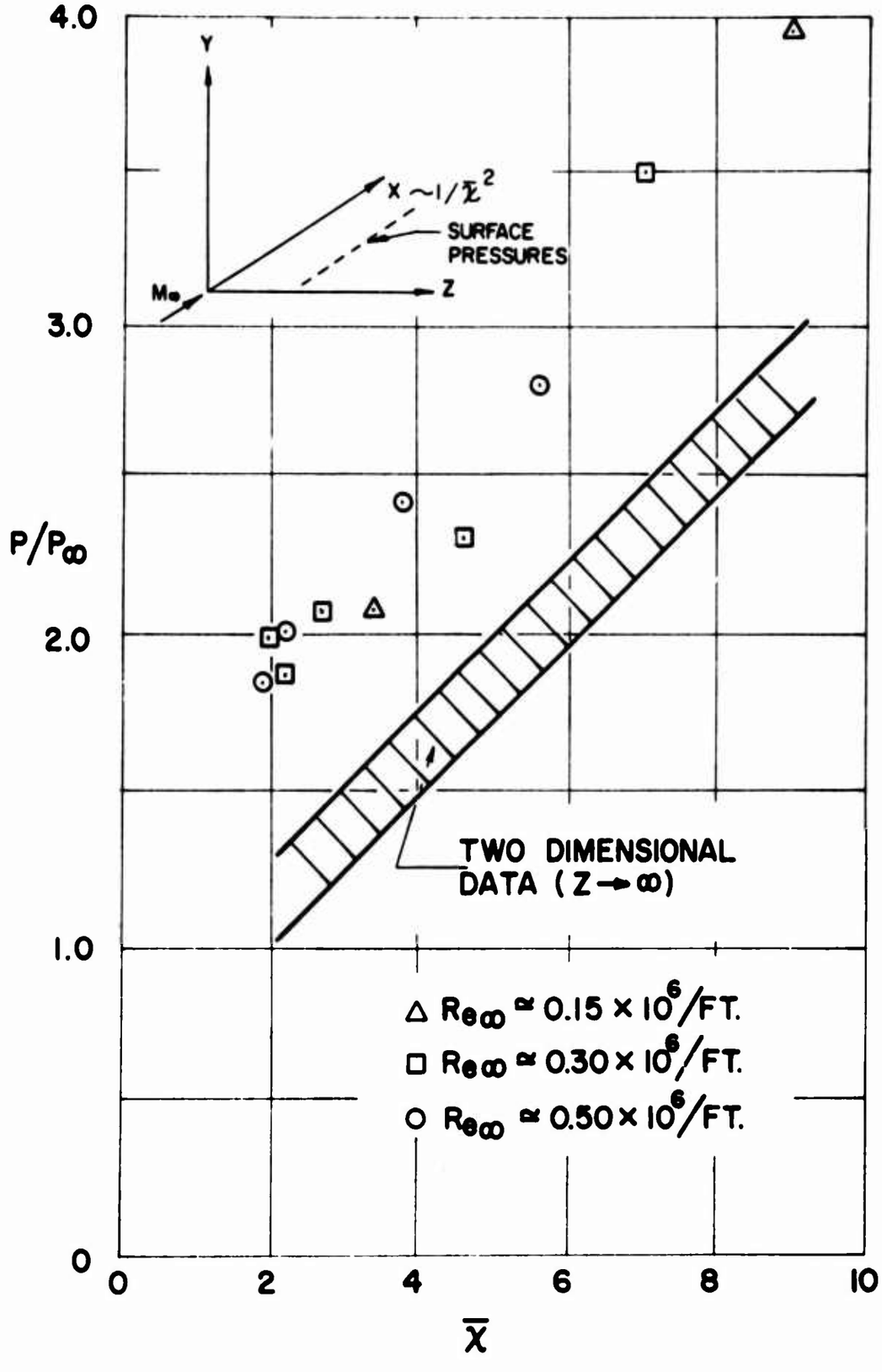

FIG. 6 SURFACE PRESSURE IN CORNER REGION.
(a) Z = 0.125 IN.

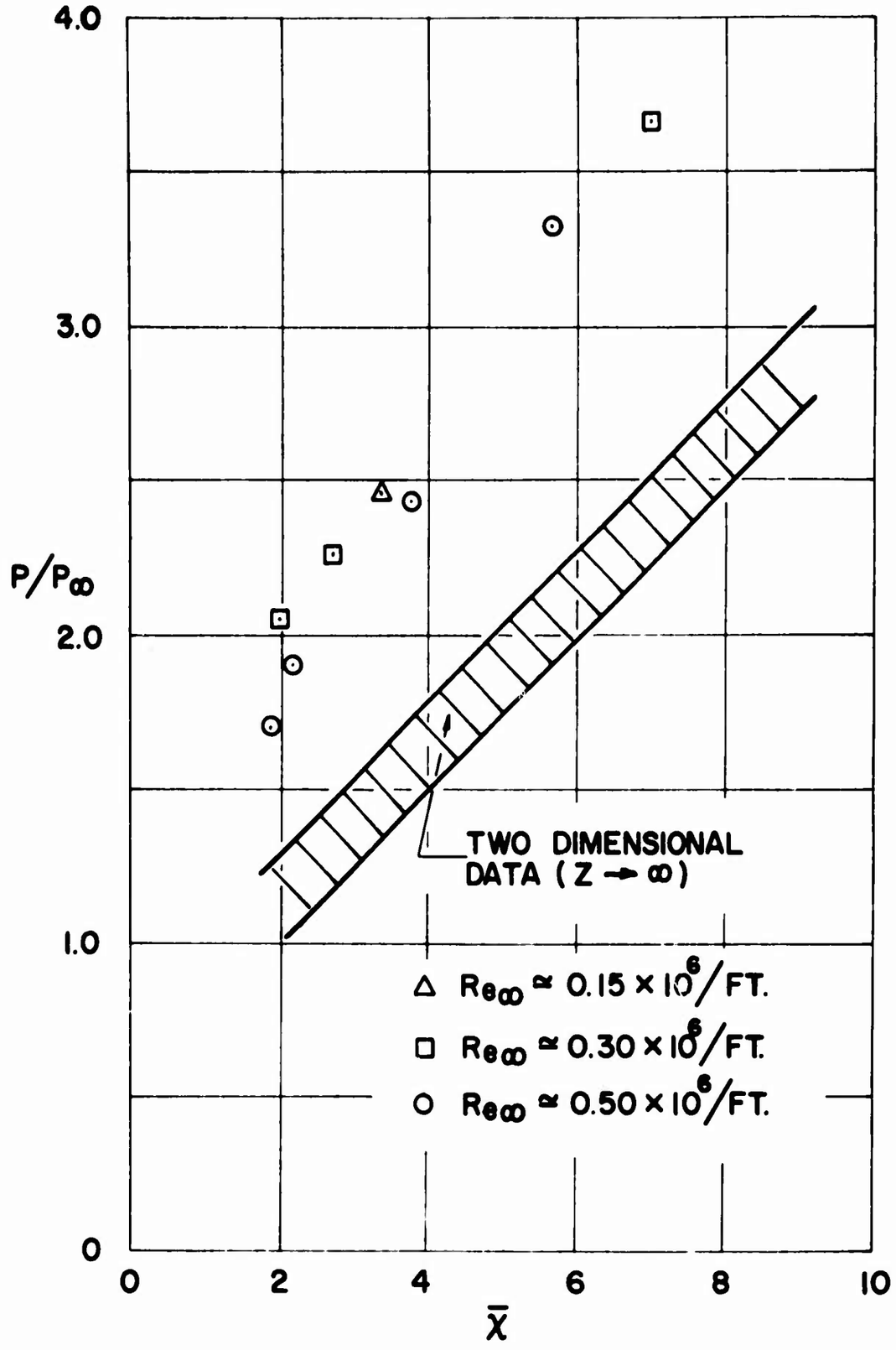

FIG. 6 SURFACE PRESSURE IN CORNER REGION
(b) Z=0.250 IN

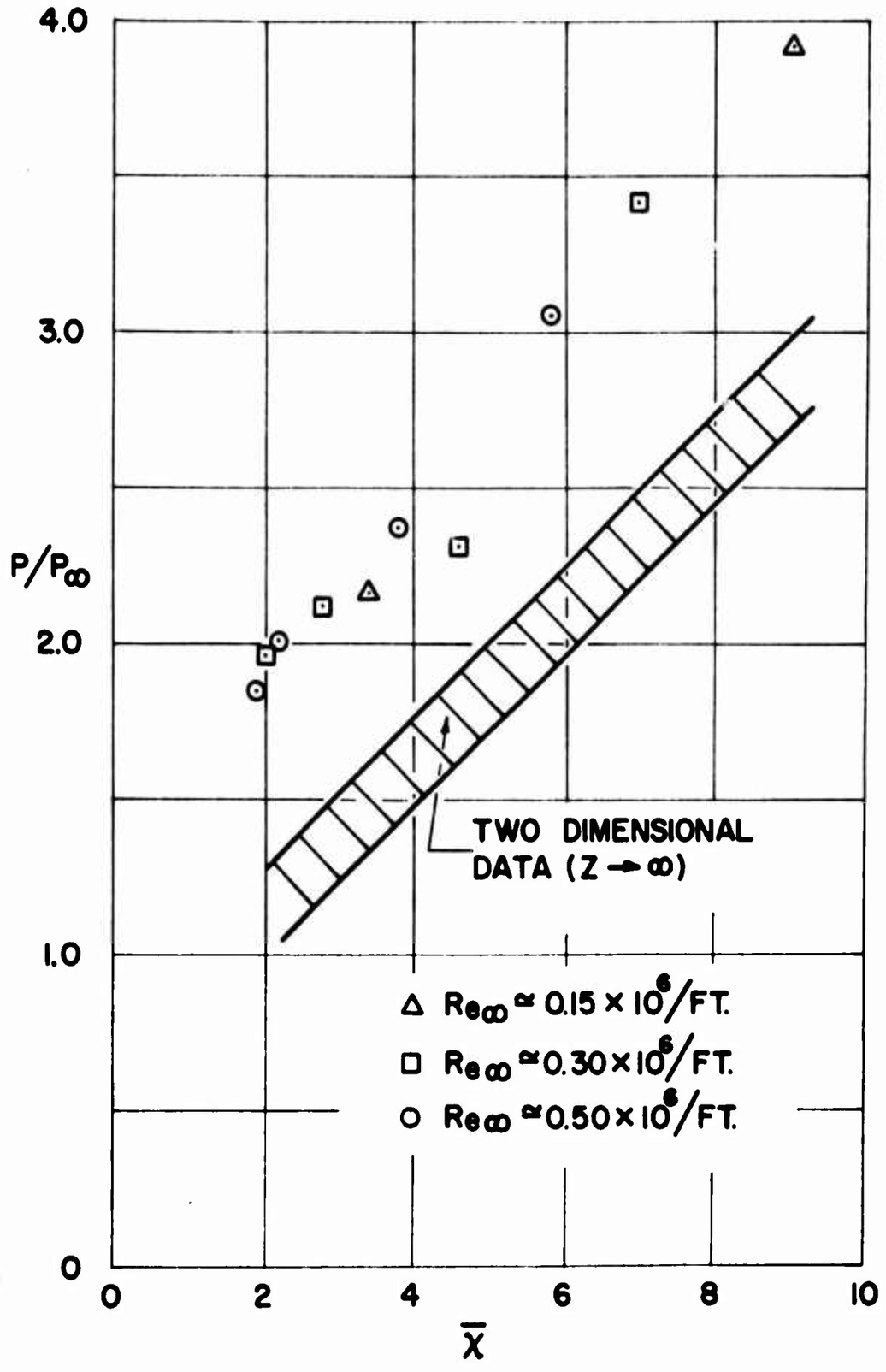

FIG. 6 SURFACE PRESSURE IN CORNER REGION
(c) Z = 0.375 IN.

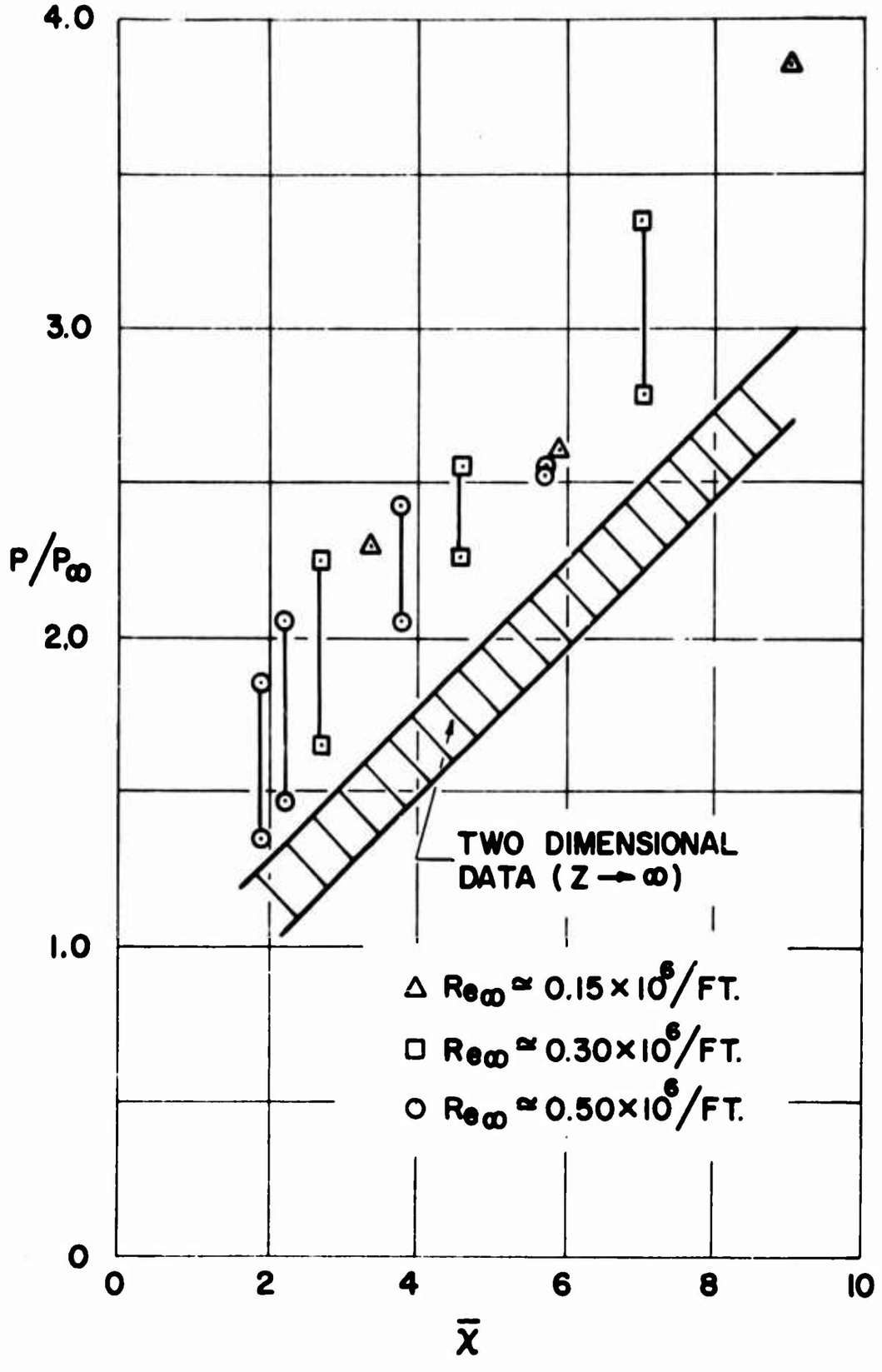

FIG. 6 SURFACE PRESSURE IN CORNER REGION
(d) Z = 0.500 IN

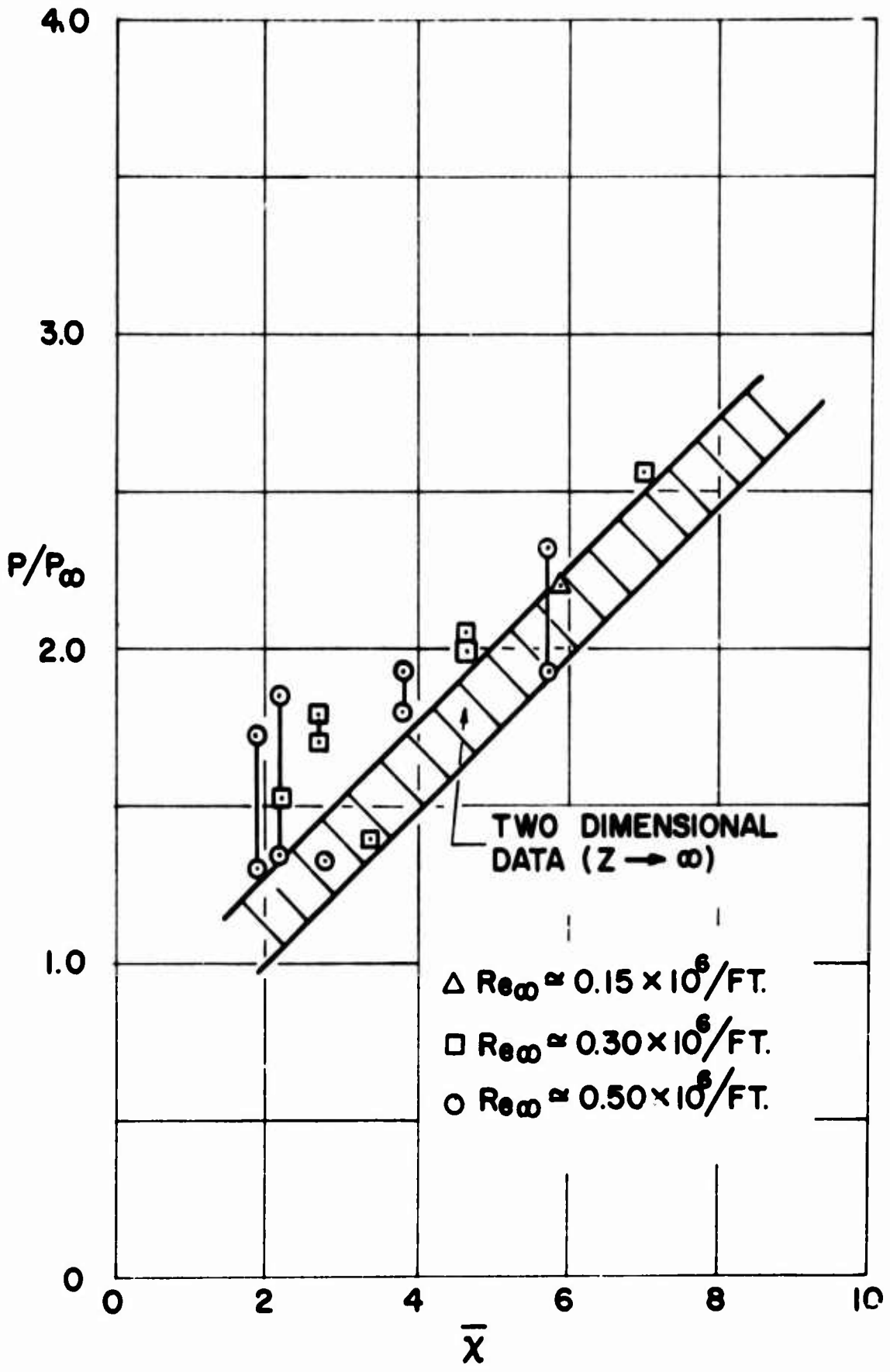

FIG. 6 SURFACE PRESSURE IN CORNER REGION
(e) Z = 1.0 IN.

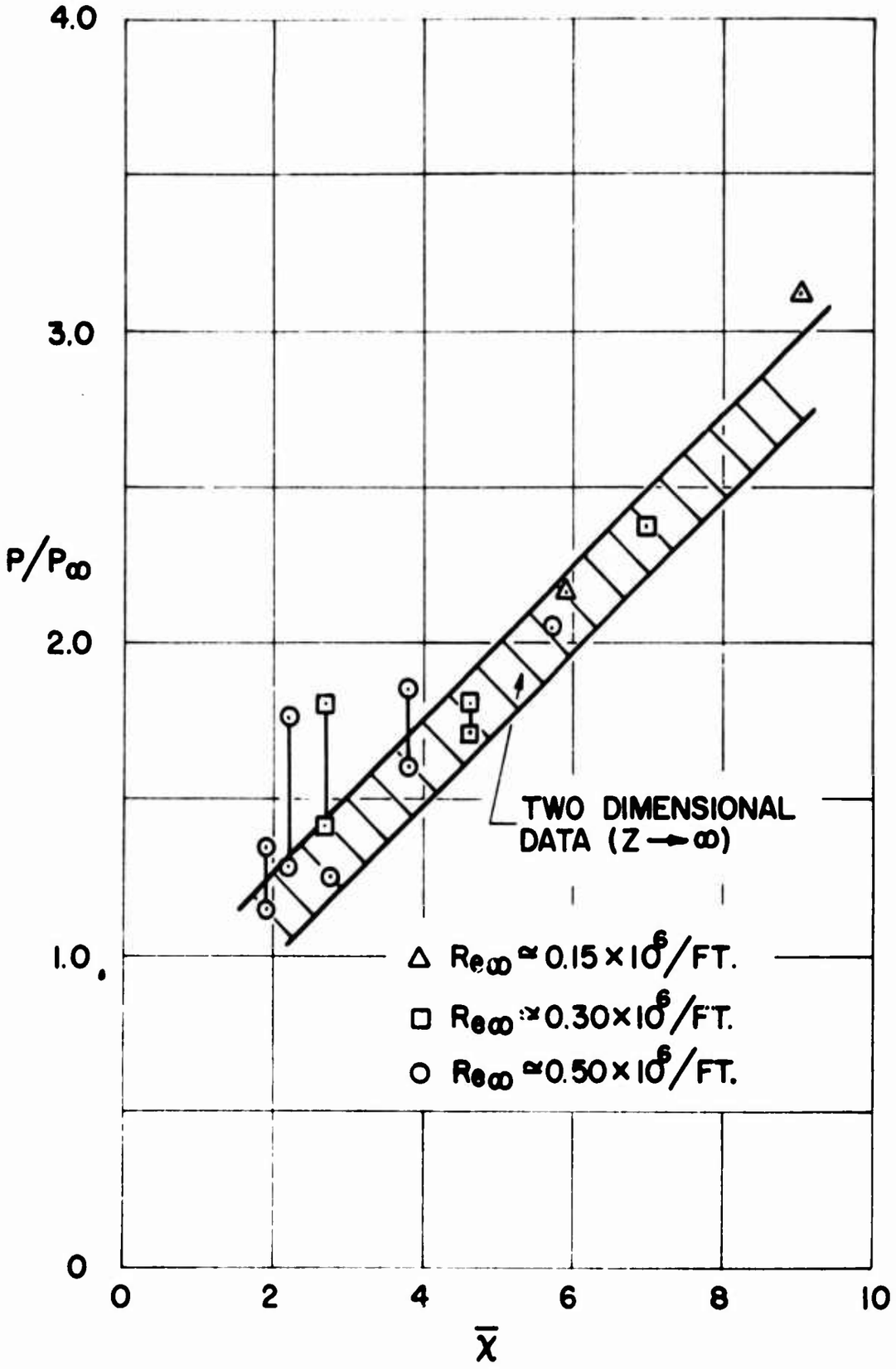

FIG. 6 SURFACE PRESSURE IN CORNER REGION
(f) Z = 1.5 IN.

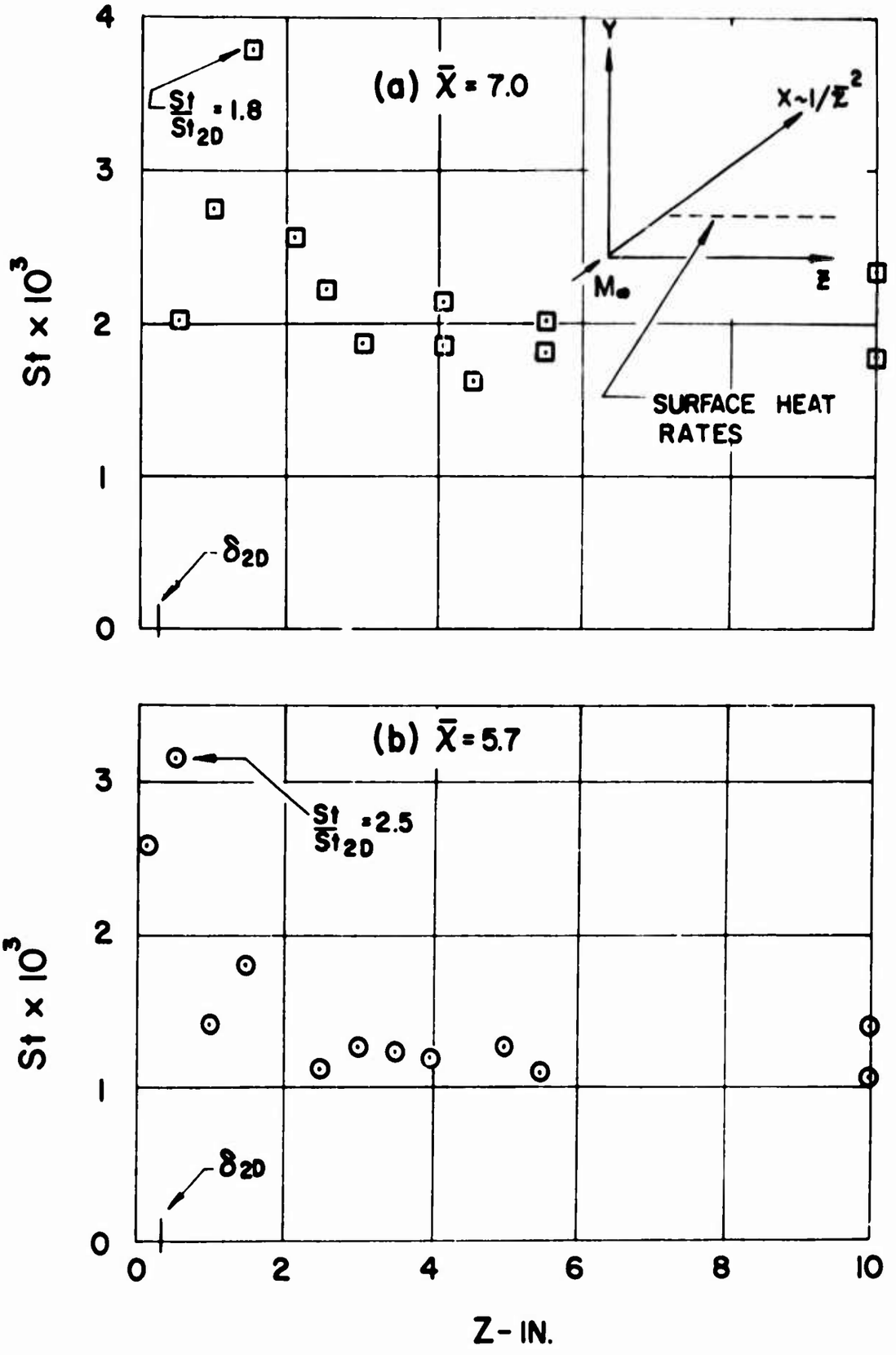

FIG. (7) LOCAL HEAT TRANSFER IN CORNER REGION

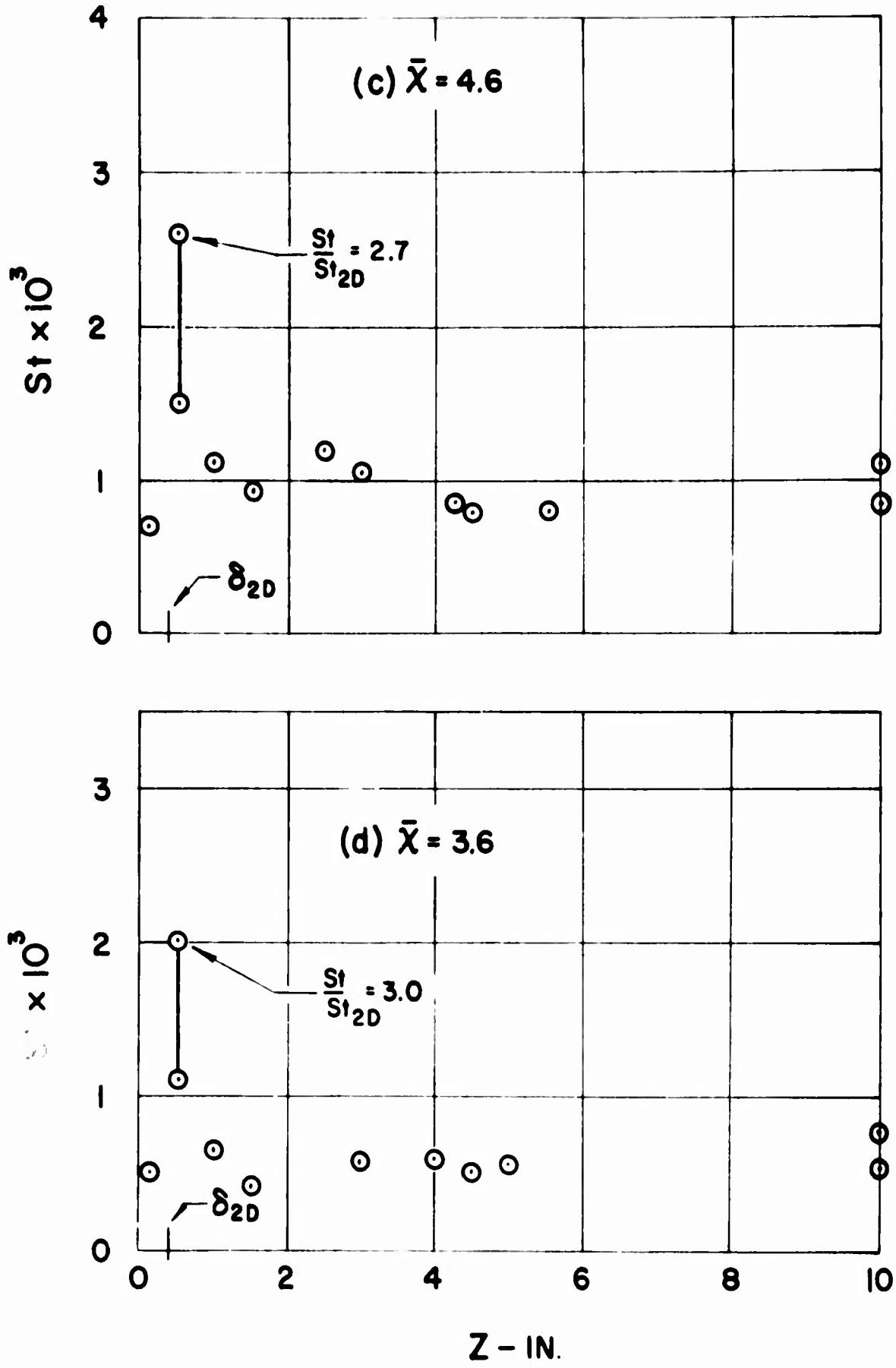

FIG. (7) LOCAL HEAT TRANSFER IN CORNER REGION

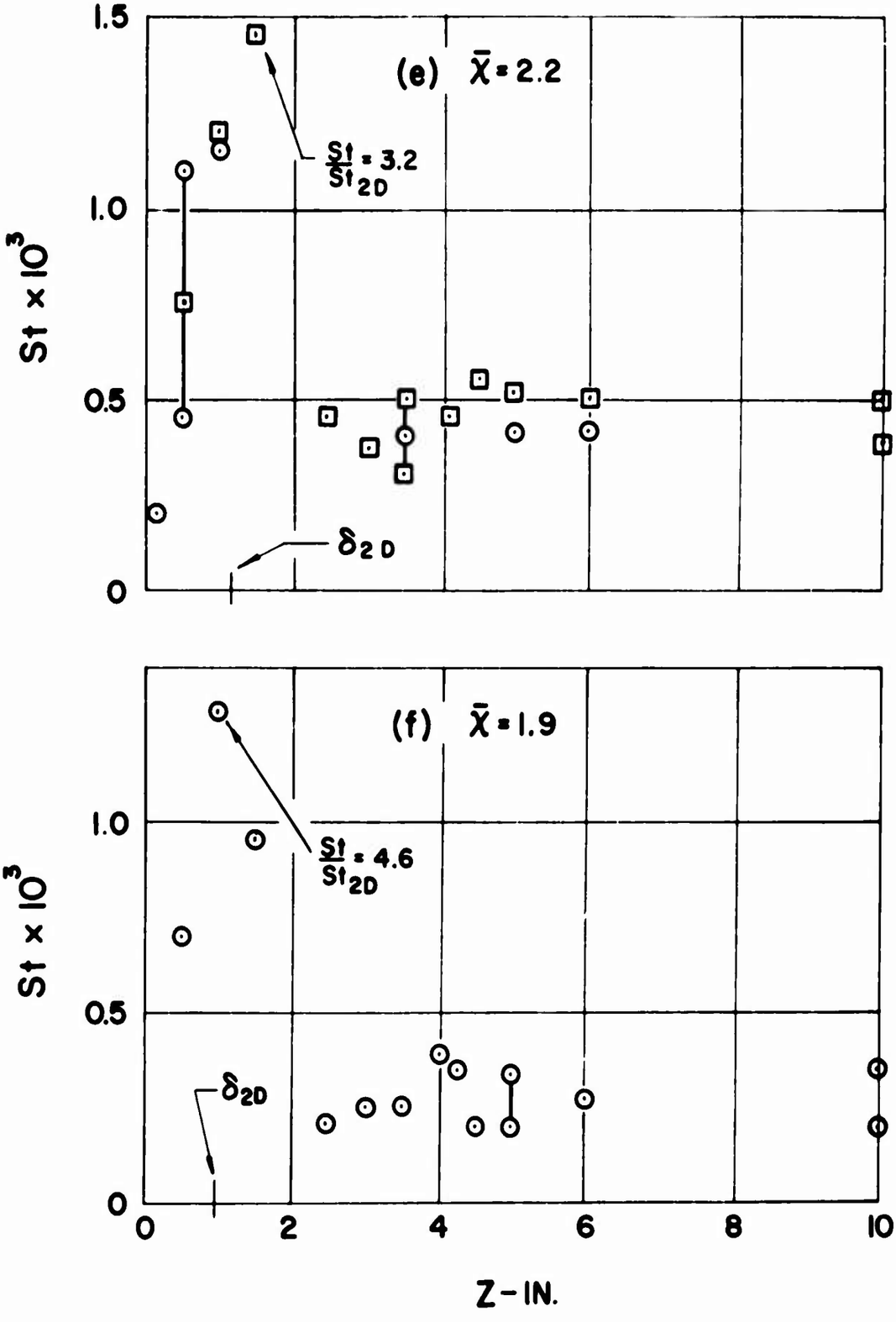

FIG. (7) LOCAL HEAT TRANSFER IN CORNER REGION

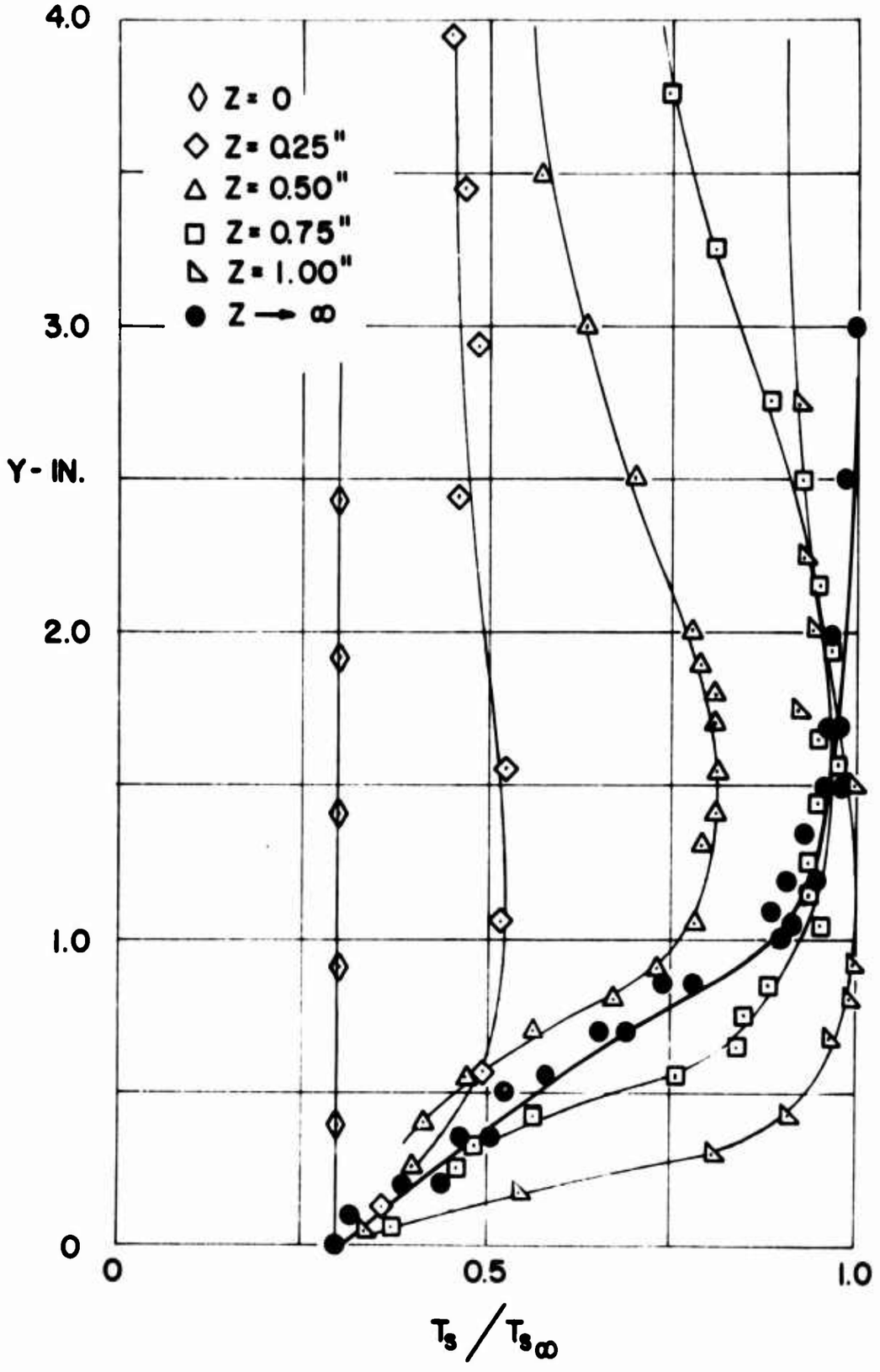

FIG. 8 TOTAL TEMPERATURE PROFILES IN CORNER REGION, $\bar{X} = 2.5$

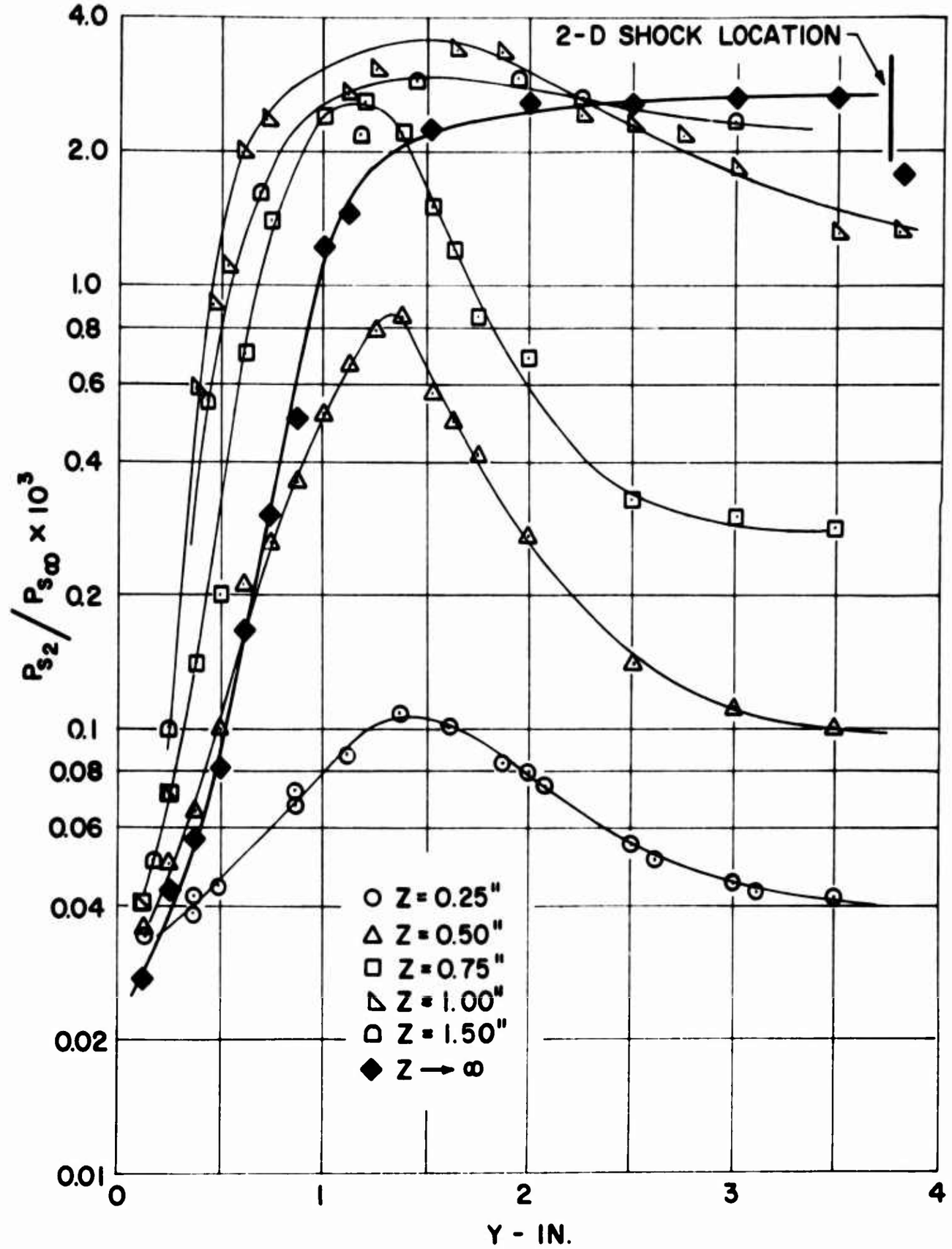

FIG. 9 PITOT PRESSURE PROFILES IN CORNER REGION, $\bar{X} = 2.5$

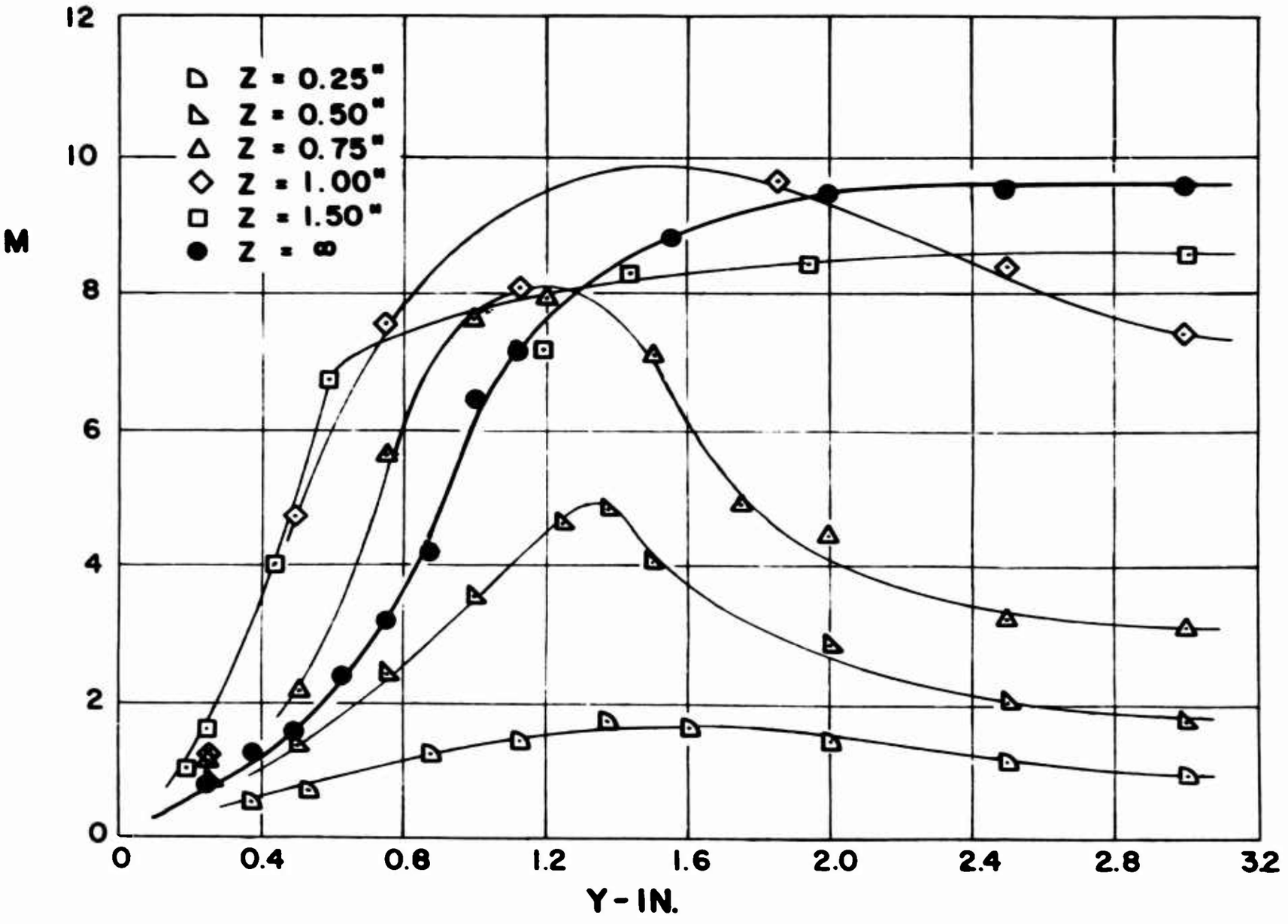

FIG. (10) MACH NUMBER DISTRIBUTION IN CORNER REGION, $\bar{X}$ = 2.5

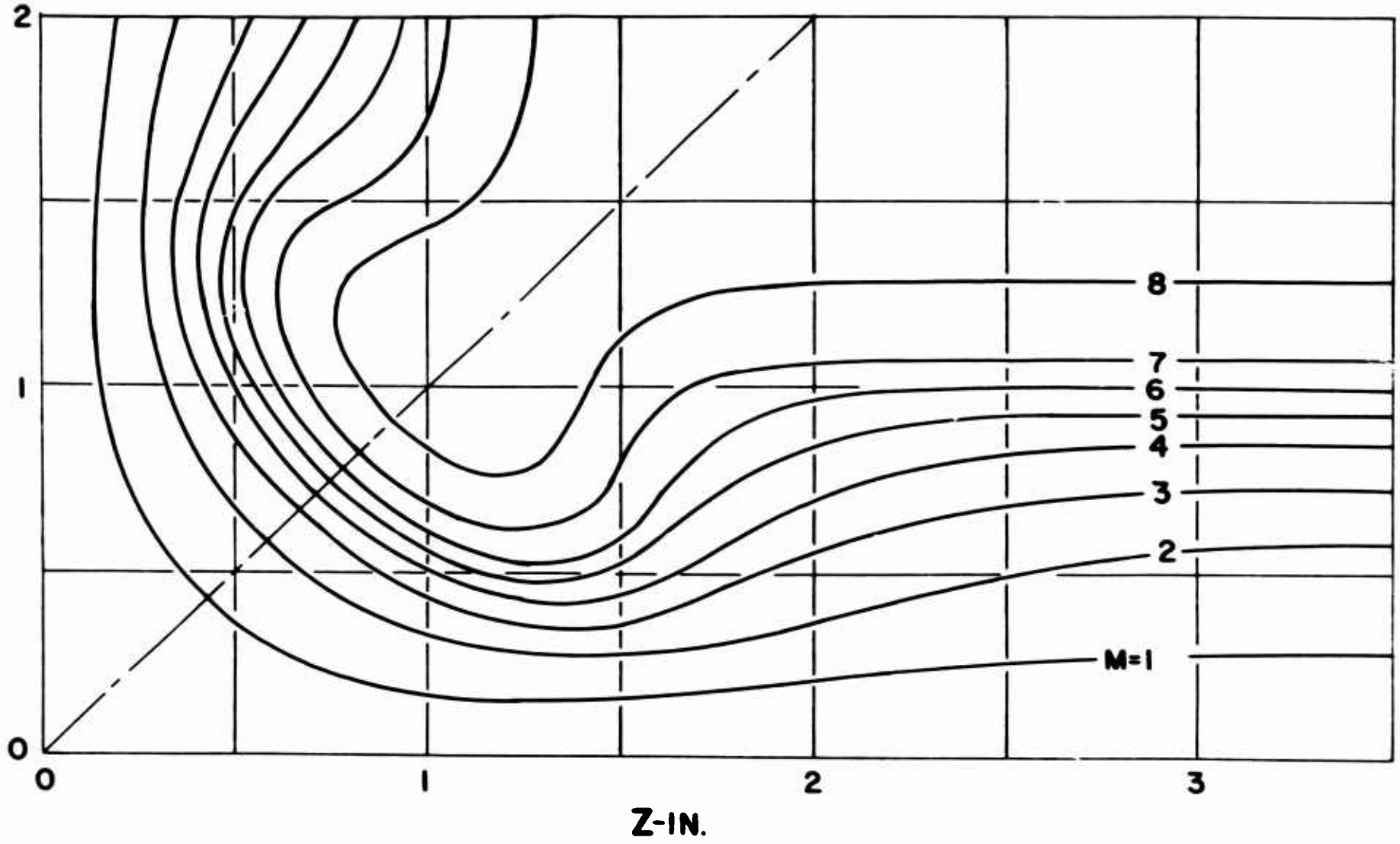

FIG. (11) MACH NUMBER CONTOURS IN CORNER REGION, $\bar{\chi} = 2.5$

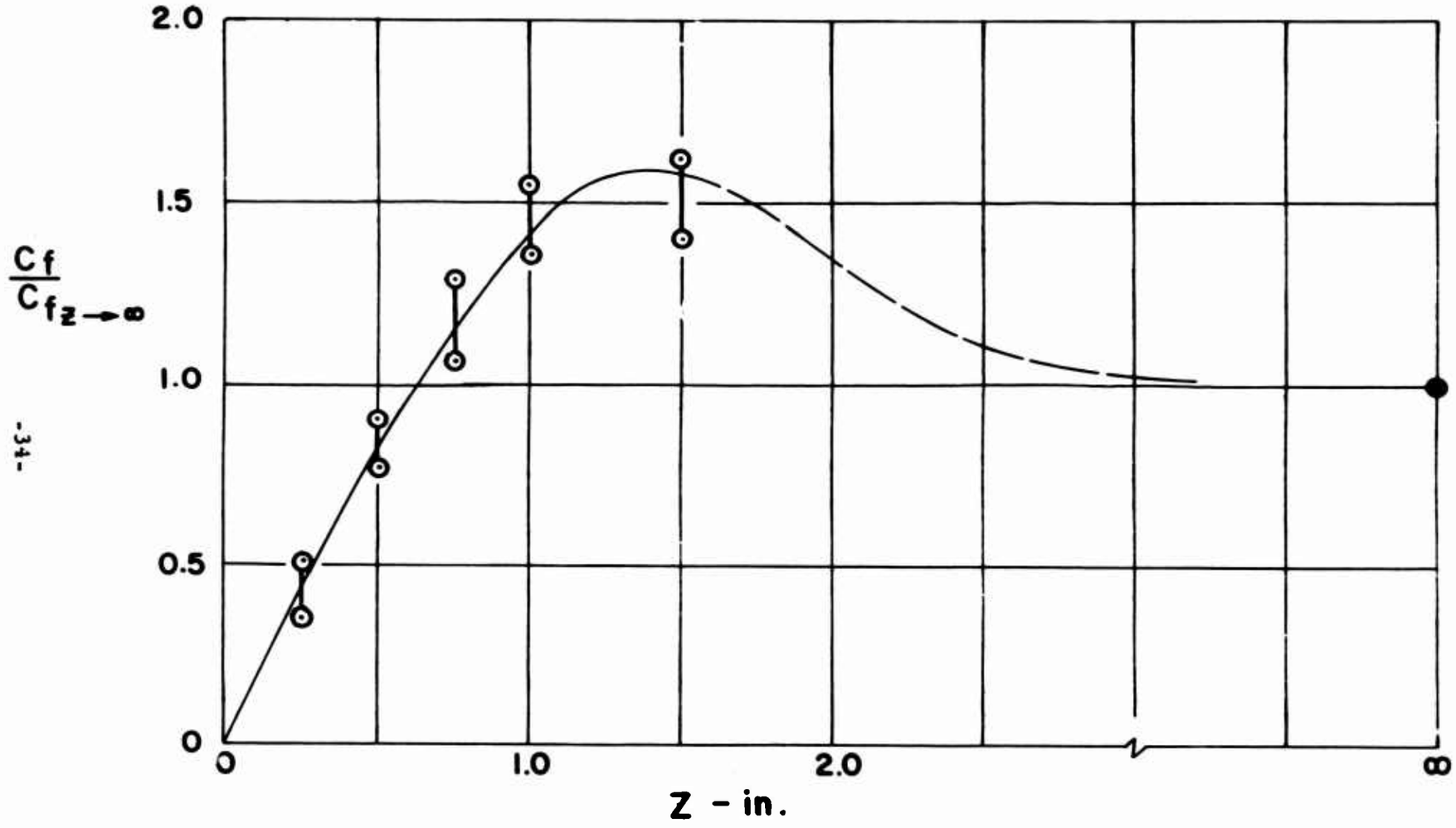

FIG (12) SKIN FRICTION VARIATION IN CORNER REGION, $\bar{X}$ = 2.5

UNCLASSIFIED
Security Classification

DOCUMENT CONTROL DATA – R&D

(Security classification of title, body of abstract and indexing annotation must be entered when the overall report is classified)

1 ORIGINATING ACTIVITY (Corporate author)

Polytechnic Institute of Brooklyn
Graduate Center
Route 110, Farmingdale, New York 11735

2A REPORT SECURITY CLASSIFICATION
☒ Unclassified
☐ Other — Specify

2B GROUP

3 REPORT TITLE

HYPERSONIC FLOW ALONG TOW INTERSECTING PLANES

4 DESCRIPTIVE NOTES (Type of report and inclusive dates)

☒ Scientific Report ☐ Final Report ☐ Journal Article ☐ Proceedings ☐ Book

5 AUTHOR(S) (Last name, first name, initial)

Cresci, Robert, J.

6 REPORT DATE AS PRINTED	7A TOTAL NO OF PAGES	7B NO OF REFS
March 1966	39	19

8A CONTRACT OR GRANT NO.
AF 49(638)-1391

B PROJECT NO.
9781-01

C 61445014

D

9A ORIGINATOR'S REPORT NUMBER(S) (If given)
PIBAL REPORT NO. 895

9B OTHER REPORT NO(S) (Any other numbers that may be assigned this report)
AFOSR 66-0500
AD

10 AVAILABILITY/LIMITATION NOTICES

Distribution of this document is unlimited

☒ Available from DDC
☐ Available from CFSTI
☐ Available from Source
☐ Available Commercially

11 SUPPLEMENTARY NOTES (Citation)

12 SPONSORING MILITARY ACTIVITY
AF Office of Scientific Research (SREM)
Office of Aerospace Research
Washington, D. C. 20333

13 ABSTRACT

The present paper deals with an experimental study of the viscous-inviscid interaction occuring in a corner region under hypersonic, low density, free stream conditions. The tests were conducted in the Mach 11.8 hypersonic tunnel at PIBAL over a range of free stream Reynolds numbers between 0.15×10^6 and 0.50×10^6/ft. The model consists of two sharp edged plates mounted at an angle of 90° with respect to each other and with normal leading edges. Data obtained include surface measurements of pressure and heat transfer for values of the interaction parameter ($\bar{\chi}$) between 1.0 and 20. The entire corner region is surveyed at a value of $\bar{\chi} = 2.5$ and measurements of total temperature, pitot, and static pressure are obtained.

The results indicate that the static pressure in the region of intersection of the shock layers is as much as twice that of the local two dimensional value. The local heat rates in this region are also considerably larger than their than their two dimensional courterparts.

DD FORM 1473
1 JAN 64

UNCLASSIFIED
Security Classification

14 KEY WORDS	LINK A		LINK B		LINK C	
	ROLE	WT	ROLE	WT	ROLE	WT
Viscous - inviscid interaction Corner flow Hypersonic flow						

INSTRUCTIONS

1. ORIGINATING ACTIVITY: Enter the name and address of the contractor, subcontractor, grantee, Department of Defense activity or other organization *(corporate author)* issuing the report.

2*a*. REPORT SECURITY CLASSIFICATION. Enter the overall security classification of the report. Indicate whether "Restricted Data" is included. Marking is to be in accordance with appropriate security regulations.

2*b*. GROUP: Automatic downgrading is specified in DoD Directive 5200.10 and Armed Forces Industrial Manual. Enter the group number. Also, when applicable, show that optional markings have been used for Group 3 and Group 4 as authorized.

3. REPORT TITLE: Enter the complete report title in all capital letters. Titles in all cases should be unclassified. If a meaningful title cannot be selected without classification, show title classification in all capitals in parenthesis immediately following the title.

4. DESCRIPTIVE NOTES: If appropriate, enter the type of report, e.g., interim, progress, summary, annual, or final. Give the inclusive dates when a specific reporting period is covered.

5. AUTHOR(S): Enter the name(s) of author(s) as shown on or in the report. Enter last name, first name, middle initial. If military, show rank and branch of service. The name of the principal author is an absolute minimum requirement.

6. REPORT DATE: Enter the date of the report as day, month, year, or month, year. If more than one date appears on the report, use date of publication.

7*a*. TOTAL NUMBER OF PAGES: The total page count should follow normal pagination procedures, i.e., enter the number of pages containing information.

7*b*. NUMBER OF REFERENCES: Enter the total number of references cited in the report.

8*a*. CONTRACT OR GRANT NUMBER: If appropriate, enter the applicable number of the contract or grant under which the report was written.

8*b*, 8*c*, & 8*d*. PROJECT NUMBER: Enter the appropriate military department identification, such as project number, subproject number, system numbers, task number, etc.

9*a*. ORIGINATOR'S REPORT NUMBER(S): Enter the official report number by which the document will be identified and controlled by the originating activity. This number must be unique to this report.

9*b*. OTHER REPORT NUMBER(S): If the report has been assigned any other report numbers *(either by the originator or by the sponsor)*, also enter this number(s).

10. AVAILABILITY/LIMITATION NOTICES: Enter any limitations on further dissemination of the report, other than those imposed by security classification, using standard statements such as

(1) "Qualified requesters may obtain copies of this report from DDC."

(2) "Foreign announcement and dissemination of this report by DDC is not authorized."

(3) "U. S. Government agencies may obtain copies of this report directly from DDC. Other qualified DDC users shall request through

_____."

(4) "U. S. military agencies may obtain copies of this report directly from DDC. Other qualified users shall request through

_____."

(5) "All distribution of this report is controlled. Qualified DDC users shall request through

_____."

If the report has been furnished to the Office of Technical Services, Department of Commerce, for sale to the public, indicate this fact and enter the price, if known.

11. SUPPLEMENTARY NOTES: Use for additional explanatory notes.

12. SPONSORING MILITARY ACTIVITY: Enter the name of the departmental project office or laboratory sponsoring *(paying for)* the research and development. Include address.

13. ABSTRACT: Enter an abstract giving a brief and factual summary of the document indicative of the report, even though it may also appear elsewhere in the body of the technical report. If additional space is required, a continuation sheet shall be attached.

It is highly desirable that the abstract of classified reports be unclassified. Each paragraph of the abstract shall end with an indication of the military security classification of the information in the paragraph, represented as *(TS)*, *(S)*, *(C)*, or *(U)*

There is no limitation on the length of the abstract. However, the suggested length is from 150 to 225 words.

14. KEY WORDS: Key words are technically meaningful terms or short phrases that characterize a report and may be used as index entries for cataloging the report. Key words must be selected so that no security classification is required. Identifiers, such as equipment model designation, trade name, military project code name, geographic location, may be used as key words but will be followed by an indication of technical context. The assignment of links, roles, and weights is optional.